Bone marrow-derived mesenchymal stem cells abate CCl4-induced lung damage *via* their modulatory effects on inflammation, oxidative stress and apoptosis

A. ADEL[1], M. ABDUL-HAMID[1], S.H. ABDEL-KAWI[2], L.O. MALLASIY[3], N.S. ABD EL-GAWAAD[4], O.M. AHMED[5]

[1]Histology and Cell Biology Division, Zoology Department, Faculty of Science, Beni-Suef University, Beni-Suef, Egypt
[2]Medical Histology & Cell Biology Department, Faculty of Medicine, Beni-Suef University, Beni-Suef, Egypt
[3]Faculty of Science and Arts in Tihama, King Khalid University, Muhayil Asir, Saudi Arabia
[4]Faculty of Science, King Khalid University, Abha, Saudi Arabia
[5]Physiology Division, Zoology Department, Faculty of Science, Beni-Suef University, Beni-Suef, Egypt

Abstract. – **OBJECTIVE:** The aim of this study was to assess and compare the therapeutic effects of allogenic and xenogeneic bone marrow-derived mesenchymal stem cells (BM-MSCs) on a rat model for treating experimental lung inflammation, oxidative stress, and apoptosis.

MATERIALS AND METHODS: Male Wistar rats were randomly divided into four groups. Group 1 received an intraperitoneal injection of olive oil vehicle (2 mL/kg body weight) for 8 weeks. Group 2 received an intraperitoneal injection of carbon tetrachloride (CCl4) (0.5 mL/kg body weight, twice/week) dissolved in olive oil for 8 weeks. Groups 3 and 4 received the CCl4 similar to group 2, followed by the intravenous injection of rat and mouse BM-MSCs (1×10^6 cells/rat twice/week into a lateral tail vein), respectively, for 4 weeks. Subsequently, the rats were sacrificed, and lung tissues were excised for molecular, histological, and ultrastructural investigations.

RESULTS: Fibrosis, interstitial bleeding, dilatation and congestion of blood vessels, intra-alveolar edema, damaged alveoli, scattered mononuclear leucocytic infiltrates, and an increased number of apoptotic cells and apoptotic remnants were observed in the lungs of rats exposed to CCl4; the treatment with rat and mouse BM-MSCs attenuated these changes. The effects of CCl4 on the increase in collagen fibers in the lungs and the expression levels of cyclooxygenase-2, tumor necrosis factor-α, and apoptotic protein p53 were considerably reduced following treatment with the BM-MSCs. The higher levels of lipid peroxidation, the lower-level glutathione content, and the activities of superoxide dismutase, glutathione peroxidase, and glutathione-S-transferase in CCl4-injected rats were significantly improved by treatments with rat and mouse BM-MSCs.

CONCLUSIONS: These findings indicate that mouse and rat BM-MSCs, which were more potent, can protect against CCl4-induced lung damage and fibrosis by reducing inflammation, apoptosis, and oxidative stress and boosting the antioxidant defense system.

Key Words:
CCl4, Lung injury, BM-MSCs, COX-2, TNF-α, p53.

Introduction

The industrial chemical carbon tetrachloride (CCl4) is used frequently to produce free radical toxicity in a range of experimental animal tissues, including the kidneys, heart, liver, lung, testis, brain, and blood[1]. After being absorbed by the skin, respiratory system, and digestive tract, it is broken down by cytochrome P-450 in the liver. Through its metabolites, the trichloromethyl free radical (CCl_3) and the trichloromethyl peroxyl radical (CCl_3O_2), it causes injury. Free radical generation in a number of organs, including the liver, kidneys, heart, lungs, brain, and blood, has been linked[2,3] to CCl4 poisoning. Lipid peroxidation (LPO) and deoxynucleic deoxyribonucleic acid (DNA) fragmentation are the results of interactions between free radicals and lipids in the lung cell membrane. A complicated interaction of oxidative stress, ne-

Corresponding Author: O.M. Ahmed, MD; e-mail: osamamoha@yahoo.com; osama.ahmed@science.bsu.edu.eg

crosis, and apoptosis is involved in the pathophysiology[4,5]. In association, glutathione reduced form (GSH) as a nonenzymatic antioxidant as well as catalase, superoxide dismutase (SOD), glutathione reductase (GR), glutathione-S-transferase (GST), and glutathione peroxide (GPx) as antioxidant enzymes are repressed[6-8]. In spite of the fact that hepatic cytochrome P450 primarily metabolizes CCl4, it caused systemic inflammation and certain organ fibrosis, including lung fibrosis in rats[9]. The lung fibrosis in rats was preceded by CCl4-induced chronic and diffuse alveolar damage and inflammation[10,11]. Thus, the CCl4-treated model was useful for the study of clinical interstitial pulmonary fibrosis accompanied by chronic inflammation[9].

Mesenchymal stem cells (MSCs) are the most thoroughly studied cells among the various stem cell groups and are widely used in regenerative medicine[12]. MSCs have many advantages since they can be obtained from a variety of sources; they can engraft and home to wounded tissues; they have a high proliferative capacity and can develop into a wide range of cell types; they have low immunogenicity and may thus be transplanted effectively across immunological barriers; and there is no ethical debate regarding the use of these cells in patients[13-15].

MSCs have been used to treat various ailments, including those that impact the neurological system, heart, liver, intestines, and lungs. MSCs can also be obtained from medical waste such as dental pulp, adipose tissue, amniotic tissue, and bone marrow[16]. MSC-based therapy is a new treatment option for lung disease. These cells colonize at the sites of lung injury, restrict the production of pro-inflammatory mediators, reduce extracellular matrix collagen deposition, and contribute to tissue repair[17-19]. Additionally, they produce paracrine factors that exhibit anti-inflammatory, anti-apoptotic, and anti-fibrotic properties[20,21].

The aim of the present study was to evaluate and compare the therapeutic effects of allogenic (rat) and and xenogenic (mice) bone marrow-derived mesenchymal stem cells (BM-MSCs) in a rat model of CCl4-induced lung injury targeting inflammation, oxidative stress, antioxidant defense system and apoptosis.

Materials and Methods

Drugs and Chemicals

CCl4 solution 99.0% was purchased from laboratory chemical trading company for laboratory fine chemicals (Cairo, Egypt). Dulbecco's modified Eagle's medium (DEMEM) was obtained from Lonza, Verviers, Belgium.

Experimental Animals

Twenty-four male adult Wistar rats weighing 120-150 g (age, 9-11 weeks) were obtained from VACSERA (Egyptian Organization for Biological Products and Vaccines), Helwan, Egypt, and fed a regular pellet diet with unlimited access to water. The animals were kept in a climate-controlled setting with a 12-hour light/dark cycle, constant temperature, and humidity. The ethical guidelines for the animal procedures were determined by the Experimental Animal Ethics Committee of the Faculty of Science at Beni-Suef University in Egypt (Ethical Approval Number BSU/FS/2019-73). Every attempt was made to limit the number of animals in this study to the bare minimum and to alleviate their misery during the experiments.

Animal Grouping

The isolation, culture, and harvesting of BM-MSCs were carried out based on the methods described by Ahmed et al[22,23], and Chaudhary and Rath[24]. BM-MSCs of rats and mice were intravenously infused into the lateral tail vein at a dose of 1 million cells/rat. The animals were randomly divided into four groups, each with six individuals (Figure 1):

Group 1 received only olive oil vehicle [2 mL/kg body weight (bw)] twice/week for 8 weeks *via* intraperitoneal injection followed by the injection of Dulbecco's Modified Eagle's Medium (DMEM) into the lateral tail vein once a week for 4 weeks.

Group 2 received CCl4 (0.5 mL/kg bw)[25] in olive oil (1.5 mL/kg; twice a week for 8 weeks) *via* intraperitoneal injection, followed by the injection of DMEM into the lateral tail vein once a week for 4 weeks.

Group 3 received CCl4 (0.5 mL/kg) dissolved in olive oil (1.5 mL/kg bw) twice/week for 8 weeks, followed by the injection of rat BM-MSCs (1 million cells/rat)[26] into the lateral tail vein (once a week for 4 weeks).

Group 4 received CCl4 (0.5 mL/kg) dissolved in olive oil (1.5 mL/kg) twice a week for 8 weeks, followed by the injection of mouse BM-MSCs (1 million cells/rat)[26] into the lateral tail veins (once a week for 4 weeks).
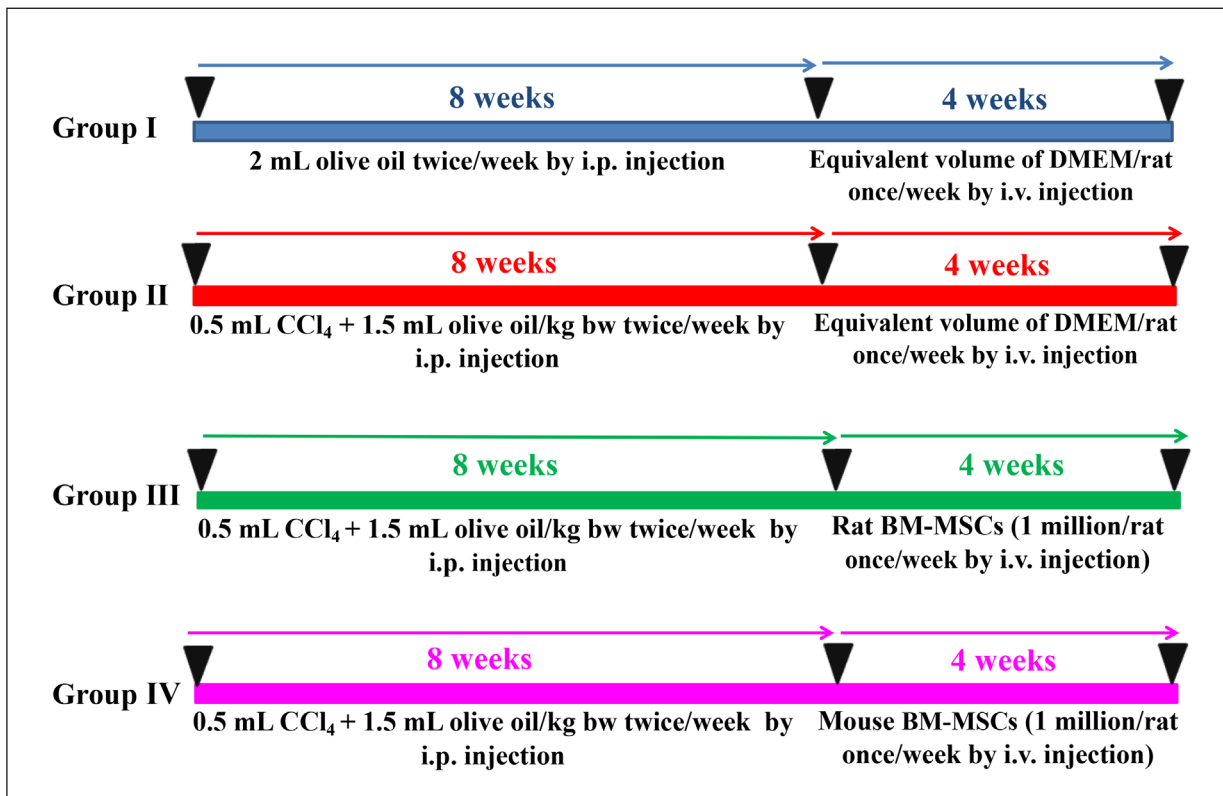
Figure 1. Schematic diagram illustrating the grouping of the animals and the experimental design.

Blood and Lung Sampling

At the end of the experiment, the rats were anesthetized by diethyl ether, and blood samples were obtained from the jugular vein. After decapitation and dissection, the lung was excised for biochemical and molecular analysis as well as for histopathological and ultrastructural investigations. One portion underwent histological analysis after being fixed in neutral buffered formalin for 24 hours, trimmed, and then transferred into 70% alcohol. Sera were rapidly separated for each individual animal and stored at -30°C until use by centrifuging at 3,000 rpm for 15 minutes to separate the serum. One gram of frozen lung tissue was homogenized in 10 ml ice-cold saline [0.9% NaCl (sodium chloride)] to yield 1% homogenate weight/volume (w/v). The supernatants were preserved at -30°C for subsequent analysis of lung antioxidant defense and oxidative stress biomarkers.

Determination of Lung Oxidative Stress and Antioxidant Biomarkers

The quantity of thiobarbituric acid reactive compounds in the lungs was measured using the Preuss et al[27] and Yagi[28] methods to determine the degree of LPO. The activities of GPx and SOD were determined based on the studies by Matkovics et al[29] and Marklund and Marklund[30], respectively. The GSH content was determined as described by Beutler et al[31], and GSH S-transferase (GST) activities were measured photometrically in the presence of GSH and 1-chloro-2,4 dinitrobenzene (CDNB), as revealed by Mannervik and Guthenberg[32].

Histological and Immunohistochemical Preparation

By the end of the experiment, the rats were euthanized by diethyl ether inhalation anesthesia and tissue samples of the lungs were excised for histopathological studies. Pieces of lungs from each animal were kept in a 10% buffered formalin solution for 48 hours before being embedded in paraffin. Following that, hematoxylin and eosin (H&E) staining of 5-μ thick sections of the paraffin-embedded lung tissues was performed. Masson's trichrome (MT) staining method was applied in lung sections to detect collagen fibers[33,34]. Immunolocalization for the detection of

cyclooxygenase (COX)-2 and apoptotic protein p53 was performed on 5-μm thick sections of the lung by the staining procedure using streptavidin-biotin-peroxidase[35]. After being deparaffinized in xylene and rehydrated in progressively stronger alcohols, the paraffin-embedded sections were rehydrated. The endogenous peroxidase and non-specific antibody binding sites were blocked by 0.3% H_2O_2 for 20 minutes and 5% normal bovine serum (1:5 diluted in TRIS solution) for 20 minutes at room temperature. Normal goat serum (10%) was applied and allowed to sit on the sections for 30 minutes to reduce non-specific binding after phosphate-buffered saline washing. The sections were incubated with anti-sera containing primary antibodies for rat tumor necrosis factor-α (TNF-α) for 1 hour (Bio Genex; Santa Cruz, CA, USA), and then for 30 min with streptavidin horseradish peroxidase (Dako-K0690, Dako Universal LSAB Kit, Dako Corporation, Carpinteria, CA, USA) and a biotinylated secondary antibody (Dako-K0690; Dako Universal LSAB Kit, Dako Corporation, Carpinteria, CA, USA). Subsequently, the sections were immunolabelled with 3, 30-diaminobenzidine tetrahydrochloride (DAB; Sigma-D5905; Sigma-Aldrich Company Ltd., Gillingham, UK) for 10 min. After that, the nuclei were stained with Harry's hematoxylin stain and the sections were dried in graded alcohol, cleaned in xylene, and mounted. For comparisons between the various experimental groups, all sections were incubated simultaneously, at the same temperature, and with the same antibody concentration. The immunohistochemically stained sections were examined under a light microscope and photographed. The microphotographs were subjected to image analysis by ImageJ software to detect the percent area and intensity of stained areas.

The stained lung sections were evaluated for the purpose of finding histological lesions. Lesions or injuries were rated as absent (0), mild (I), moderate (II), and severe (III) for alterations, in three randomly chosen fields of each section (×100)[36]. Necrosis, thickening of the interalveolar septum, apoptosis, and collagen fibers were among the graded lesions.

Electron Microscopy

The lung samples were divided into pieces measuring about 1 mm³ and preserved in fresh glutaraldehyde-formaldehyde solution at a concentration of 3% for 18 to 24 hours at 4°C. They were then post-fixed for an hour at 4°C in osmium tetroxide after being washed in phosphate buffer (pH 7.4). The specimens were then dehydrated in ascending concentrations of ethanol. After that, the samples were submerged in propylene oxide solution twice for 10 minutes each. The specimens were transferred to capsules containing fresh resin the next day and polymerized for one day in a 60°C oven, resulting in hard blocks. The ultra-microtome glass knives were then used to cut ultrathin sections that were colored with uranyl acetate and lead citrate and inspected using a Joel CX 100 transmission electron microscope (Joel, Tokyo, Japan) with a 60 kV accelerating voltage[37].

Evaluation of Immunohistochemical Staining Intensity

The percentages of COX-2, TNF-α, and p53 immuno-reactive cells in the sections were calculated using the "Leica Quin 500C" image analyzer computer system (Leica Imaging System Ltd., Cambridge, England); three images were examined from each group. The ImageJ software is beneficial for evaluating immunohistochemically stained specimens because the method is more accurate and repeatable than the traditional counting method. The total positively-stained (brown) and negatively-stained (blue) areas can be picked using the thresholding tool and the "area technique." The positive immunohistochemistry index can be calculated using this data.

Statistical Analysis

For the statistical analysis, the Statistical Package of Social Sciences (SPSS) program version 21 (IBM Corp., Armonk, NY, USA) was utilized. The mean and standard error (SE) are used to express all values. To identify significant differences between the groups, a one-way analysis of variance and Duncan's multiple-range test were employed[38]. Values of $p < 0.05$ were regarded as significant.

Results

Effects on Lung Oxidative Stress and Antioxidant Defense System

The treatment of CCl4-induced rats produced a significant decrease in the formation of malondialdehyde (MDA) in the lungs by rat and mouse BM-MSCs, as indicated in Table I. The activity of lung SOD was significantly decreased in the CCl4-treated animals when compared to that in

Table I. Effects on lung SOD activity and LPO.

Groups	SOD (U/mg tissue)	% change	LPO (nmol/100 mg tissue)	% change
Control group	126.23 ± 0.77^d		11.81 ± 0.31^a	
CCl4 group	61.68 ± 1.58^a	-51.14	26.13 ± 1.57^d	121.25
CCl4 + rat BM-MSCs	102.45 ± 3.54^c	66.09	14.62 ± 0.12^b	-44.05
CCl4 + mouse BM-MSCs	78.85 ± 3.03^b	27.84	17.78 ± 0.36^c	-31.96
F-probability			$p > 0.05$	

Results are displayed as mean ± SE. There are six animals in each group. Mean values with different superscript letters are significantly different at $p < 0.05$. [a,b,c,d]Indicated the similarity or difference between groups. Lipid peroxidation (LPO), bone marrow-derived mesenchymal stem cells (BM-MSCs), superoxide dismutase (SOD).

the control group (Group 1). However, treatment with BM-MSCs resulted in a significant increase in SOD activity (Table I).

Table II shows the concentrations of GSH in the lung homogenates. A significant ($p < 0.05$) depletion in the concentration of GSH was noticed in the CCl4-treated rats in comparison with the control group. Furthermore, the GST activity was significantly decreased in the lung tissue homogenates of the CCl4-treated rats compared to those of the control rats; the activity was restored following treatment with the rat and mouse BM-MSCs (Table II). Likewise, the GPx activity was significantly diminished in the CCl4-injected rats in comparison with the control rats. Treatment with BM-MSCs significantly reduced the enzyme activity in the lung tissue homogenates; furthermore, treatment with rat BM-MSCs was more effective than that with mouse BM-MSCs (Table II).

Lung Histological Changes

Staining with H&E revealed the normal architectural appearance of the lung tissues in the Group 1 rats, with normal clear alveoli that were separated by thin inter-alveolar septa (Figure 2a). After injection with CCl4, alveolar edema with thickening of the alveolar walls (Figure 2b-c), hemorrhage, cellular mononuclear leucocytic infiltration, damaged alveoli (Figure 2c-e), and fibrosis (Figure 1d-e) in addition to many apoptotic cells and apoptotic bodies or remnants and necrosis (Figure 2b-e) were observed in the rats in Group 2. The sections from Group 3 (treated with rat BM-MSCs) showed restoration of the lung structure (Figure 2f), whereas those from Group 4 (treated with mouse BM-MSCs) showed a rupture of the alveolar walls (Figure 2g). The severity of tissue damage in Group 4 was higher than that in Group 3, suggesting that rat BM-MSCs provide higher protection than mouse BM-MSCs. Few apoptotic cells were noticed in Groups 3 and 4.

MT staining of the lung sections was performed to assess the extracellular matrix depositions (Figure 3). All control animals revealed a normal distribution of blue-stained collagen fibers in the lung tissues (Figure 3a), whereas

Table II. Effects on lung GSH content and GST and GPx activities.

Groups	GSH (nmol/100 mg tissue)	% change	GST (U/100 mg tissue)	% change	GPx (mU/100 mg tissue)	% change
Normal group	18.85 ± 0.48^d		93.49 ± 0.79^d		138.07 ± 0.35^d	
CCl4 group	10.37 ± 0.27^a	-44.99	53.48 ± 1.54^a	-42.79	99.16 ± 3.68^a	-28.18
CCl4 + rat BM-MSCs	15.02 ± 0.47^c	44.84	85.05 ± 1.22^c	59.03	123.95 ± 0.62^c	25.00
CCl4 + mouse BM-MSCs	12.55 ± 0.41^b	21.02	64.33 ± 0.43^b	20.29	113.19 ± 0.66^b	14.15
F-probability			$p > 0.05$			

Results are displayed as mean ± SE. There are six animals in each group. Mean values with different superscript letters are significantly different at $p < 0.05$. [a,b,c,d]Indicated the similarity or difference between groups. Bone marrow-derived mesenchymal stem cells (BM-MSCs), glutathione reduced form (GSH), glutathione-S-transferase (GST), and glutathione peroxide (GPx).
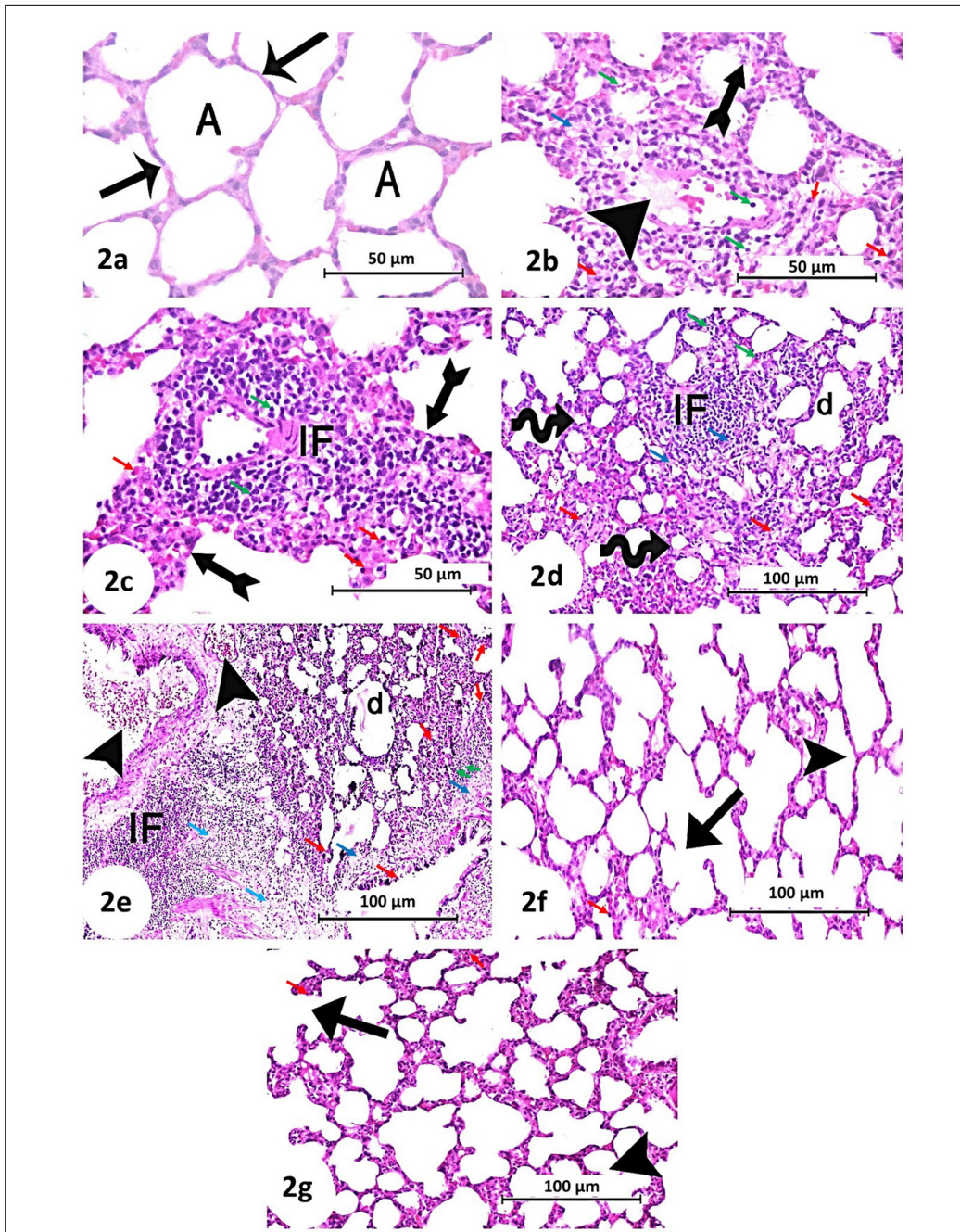
Figure 2. Photomicrographs of lung section of rats showing (**a**): the normal architecture of the lung tissue, normal clear alveoli (A), and thin inter-alveolar septa (*long arrow*) (Scale bars of **a** = 50 μm). **b-c**, CCl4-treated group shows loss of normal architecture of the lung tissue, with diffused mononuclear leucocytic infiltration (IF) associated with necrotic areas (*blue arrows*) appearing within the inter-alveolar septa, extensive thickening of interalveolar septa (*bifid arrow*) and dilated congested pulmonary blood vessels (*arrowhead*) in addition to the presence of many apoptotic cells (*red arrows*) and apoptotic bodies or remnants (*green arrows*) (Scale bars of **b-c** = 50 μm). **d-e**, Lung section of the CCl4-treated group shows diffused inflammatory mononuclear leucocytic infiltration (IF) associated with necrotic areas (*blue arrows*), collapsed alveoli (wave arrow), while the neighboring ones are irregularly dilated (**d**) and dilated congested blood vessels (*arrowhead*) (Scale bars of **d-e** = 100 μm). Many apoptotic cells (*red arrows*) and apoptotic bodies or remnants (*green arrows*) were also observed. **f**, Lung section of CCl4-treated group showing CCl4 + rat BM-MSCs and (**g**): CCl4 + mouse BM-MSCs showing rupture of alveolar walls (long black arrow), somewhat thin inter-alveolar septa (*arrowhead*) and amelioration of structure pulmonary tissue. Few apoptotic cells (*red arrows*) and apoptotic bodies or remnants (*green arrows*) were also observed. (H&E stain; Scale bars of **f-g** = 100 μm).
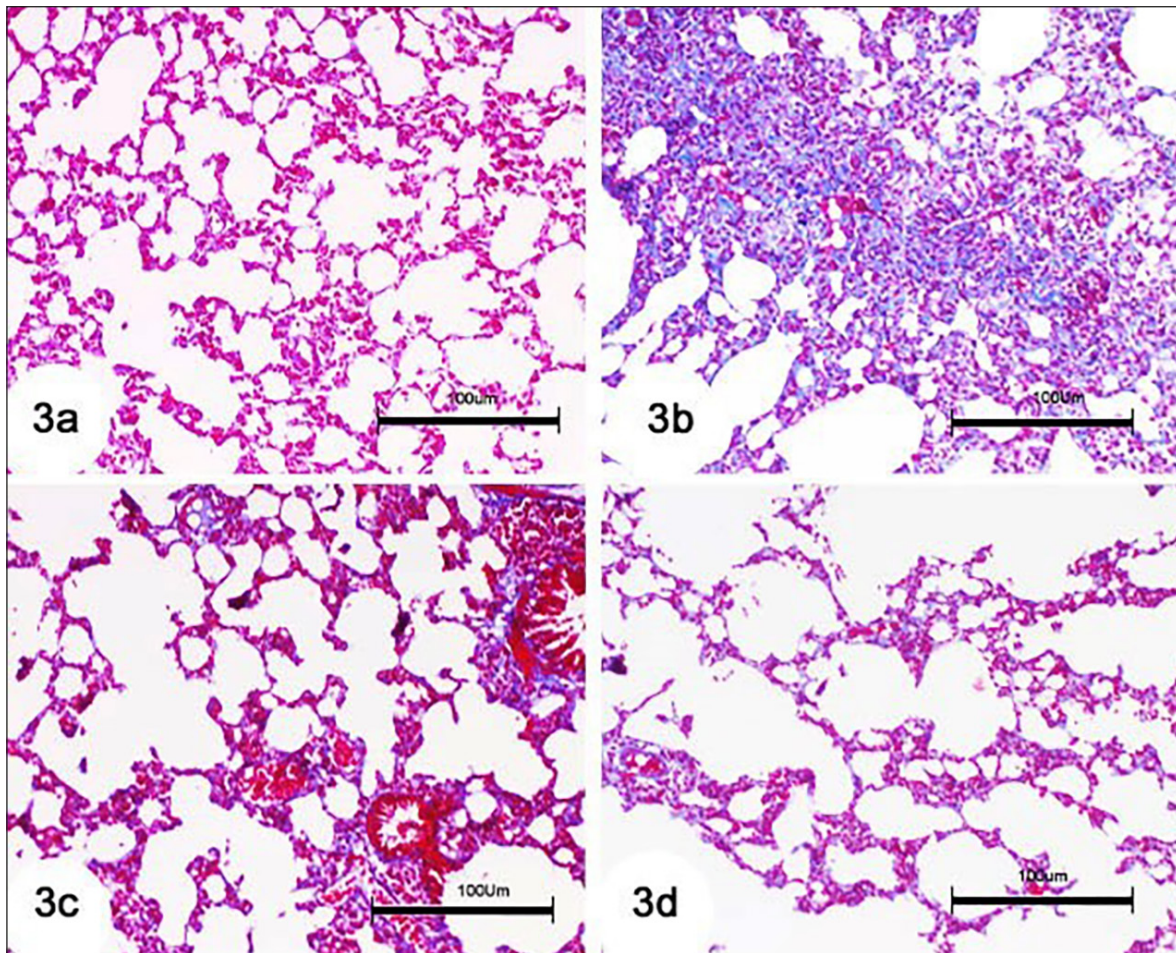
Figure 3. Photomicrographs of lung section of rats showing (**a**): normal distribution of little collagen fibers in control lung tissues. **b**, CCl4-treated group showing significantly increased stained blue collagen fibers in lung tissues. **c**, CCl4 + rat BM-MSCs and (**d**): CCl4 + mouse BM-MSCs showing significantly decreased stained blue collagen fibers compared with group CCl4. [Masson's trichrome stain; Scale bars of (**a-d**) = 100 μm].

the CCl4-treated rat lungs showed a significant increase in collagen fibers (Figure 3b). The extent of staining of the collagen fibers in Groups 3 and 4 was significantly lower than that in Group 2 (Figure 3c-d). Histopathological change scores of different groups are represented in Table III. The normal control lung section showed no histological lesions, as shown by a zero score. CCl4-treated rats demonstrated different grades of histopathological alterations scores of lungs ranging from grade III to grade 0. The treatments of the CCl4-injected group with mice BM-MSCs and rats' BM-MSCs illustrated marked amelioration in histological lesions, including necrosis, thickening of interalveolar septa, apoptosis, and collagen fibers as compared with the CCl4-injected group.

Effects on Lung COX-2, TNF-α and p53 Protein Expressions

Negative immunoreaction for COX-2 was observed in the control group (Figure 4a), whereas in group 2, the pulmonary cells were positively stained (Figure 4b). Weak immunoreactions were observed in the lungs of rats in groups 3 and 4 (Figure 4c-d).

Negative immunoreaction for TNF-α in pulmonary cells was noticed in the control group (Figure 5a); however, it was strongly positive in hyperplastic alveolar or bronchial epithelial cells (Figure 5b) in the CCl4 group. On the other hand, weak immunoreactions for TNF-α in pulmonary cells were depicted in CCl4 groups treated with rat and mouse BM-MSCs (Figure 5c-d).

Table III. Histopathological scores of lung lesions in normal control, CCl4, CCl4/rat BM-MSCs, CCl4/mouse BM-MSCs groups.

Histopathological changes	Score	Normal control	CCl4	CCl4/rat BM-MSCs	CCl4/mouse BM-MSCs
Necrosis	0	6 (100%)	1 (16.7%)	6 (100%)	5 (83.3%)
	I	—	1 (16.7%)	—	1 (16.7%)
	II	—	1 (16.7)	—	—
	III	—	3 (50%)	—	—
Thickening of interalveolar septa	0	6 (100%)	—	5 (83.3%)	4 (66.7%)
	I	—	1 (16.7%)	1 (16.7%)	1 (16.7%)
	II	—	2 (33.3%)	—	1 (16.7%)
	III	—	3 (50.0%)	—	—
Mononuclear leucocytic infiltration (Inflammation)	0	6 (100%)	—	6 (100%)	6 (100%)
	I	—	—	—	—
	II	—	2 (33.3%)	—	—
	III	—	4 (66.7%)	—	—
Apoptosis	0	6 (100%)	—	5 (83.3%)	5 (83.3%)
	I	—	1 (16.7%)	1 (16.7%)	—
	II	—	2 (33.3%)	—	1 (16.7%)
	III	—	3 (50.0%)	—	—
Collagen fibers	0	6 (100%)	—	4 (66.7%)	4 (66.7%)
	I	—	—	1 (16.7%)	—
	II	—	2 (33.3%)	1 (16.7%)	2 (33.3%)
	III	—	4 (66.7%)	—	—

Histopathological lesions were rated as absent (0), mild (I), moderate (II), and severe (III).
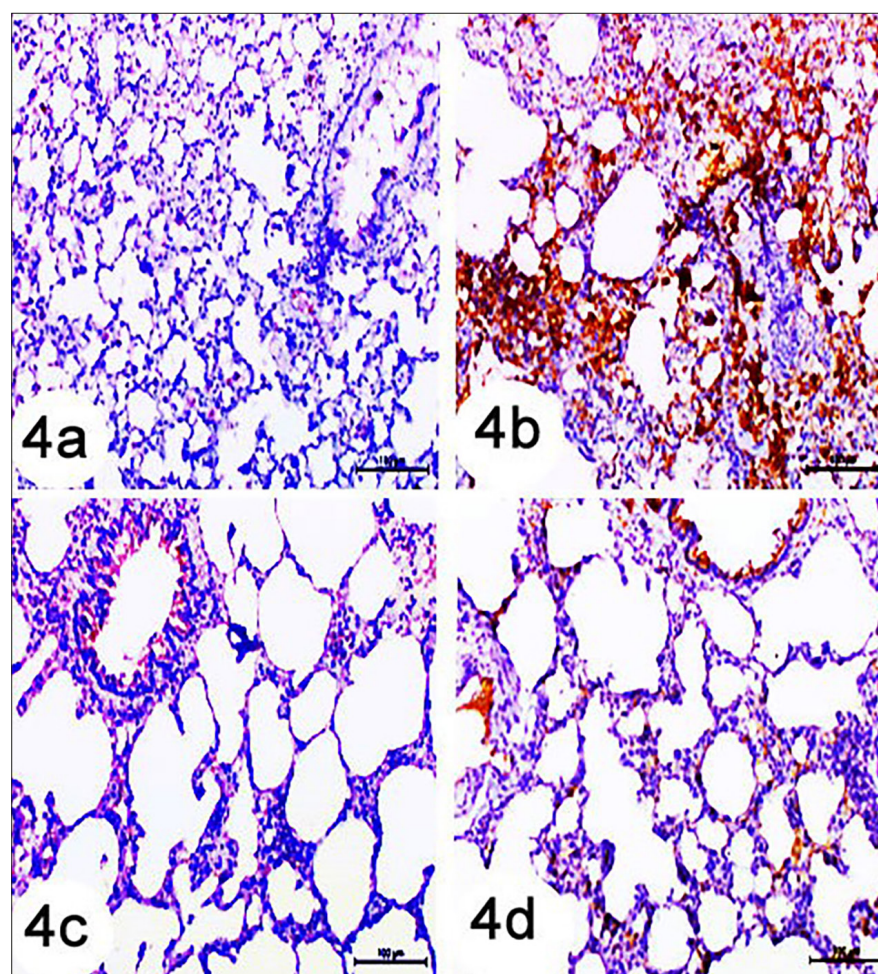
Figure 4. Photomicrographs of lung section of rats showing (**a**): normal control group with the negative immune reaction for COX-2 in pulmonary cells. **b**, Group CCl4 showing strong brown positive immune reaction for COX-2 in the bronchiolar epithelial cells and alveolar septum. **c**, CCl4 + rat BM-MSCs and (**d**): CCl4 + mouse BM-MSCs showing few immune reactions for COX-2 in the bronchiolar epithelial cells and alveolar septum. [Immunostaining for COX-2; Scale bars of (**a-d**) = 100 μm].

11390

Figure 5. Photomicrographs of lung section of (**a**): rats of control group showing negative reaction for TNF-α in pulmonary cells. **b**, Group CCl4 showing intense positive immune reaction for TNF-α in pulmonary cells. **c**, CCl4 + rat BM-MSCs and (**d**): CCl4 + mouse BM-MSCs showing weak immunoexpression for TNF-α in pulmonary cells. [Immunostaining for TNF-α; Scale bars of (**a-d**) = 50 μm].
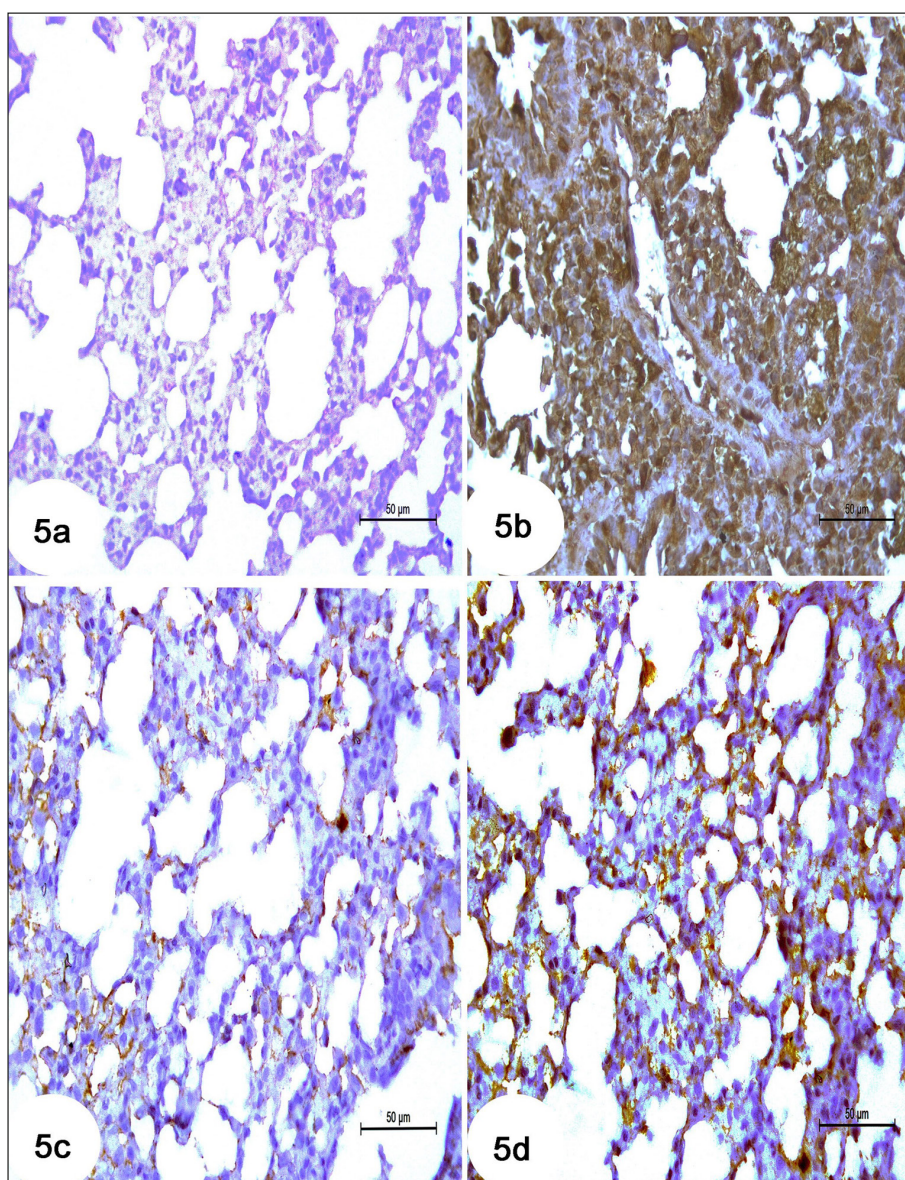
Similar to COX2 and TNF-α, negative immunoreaction for p53 in pulmonary cells was shown in the control group (Figure 6a), whereas, in group 2, the hyperplastic alveolar or bronchial epithelial cells were positively stained (Figure 6b). Weak staining was observed in the lung cells of animals in groups 3 and 4 (Figure 6c & d). The data obtained by immunohistochemical investigation in Table IV showed a significant increase ($p < 0.05$) in the expression levels of COX-2, TNF-α, and p53, observed after CCl4 injection. Treatment of the CCl4-injected rats with rat and mouse BM-MSCs produced a significant decrease ($p < 0.05$) in these proteins. Treatment with rat BM-MSCs was more effective than that with mouse BM-MSCs. The image and statistical analysis of COX-2, TNF-α, and p53 indicated a significant increase in the brown color intensity in the CCl4 group compared to CCl4 groups treated with rat and mouse BM-MSCs (Table IV).

Ultrastructural Changes

Transmission electron microscopy (TEM) of the lung tissue from the control group (Figure 7a-b) revealed normal alveolar structures with type II pneumocytes consisting of a large, rounded nucleus and numerous cytoplasmic organelles, including lamellar inclusion bodies and microvilli on the free border facing the alveolar space. The
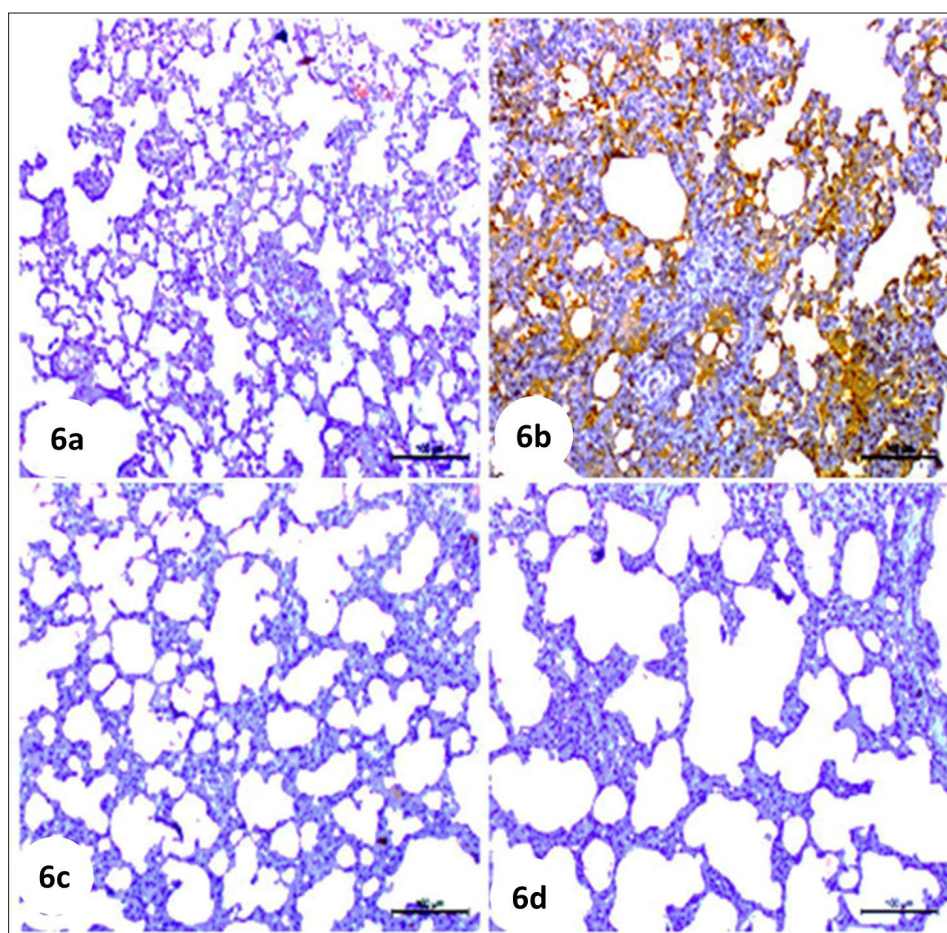
Figure 6. Photomicrographs of lung section of (**a**): rats of control group showing normal negative immune reaction for p53 in pulmonary cells. **b**, Group CCl4 showing intense positive immunoreaction for p53 in pulmonary cells. **c**, CCl4 + rat BM-MSCs and (**d**): CCl4 + mouse BM-MSCs showing weak immunoexpression for p53 in pulmonary cells. [Immunostaining for p53; Scale bars of (**a-d**) = 100 μm].

lung tissues from group 2 showed type II pneumocytes, which had vacuolated lamellar bodies and a shrunken, black, eccentric nucleus. The capillary basement membrane seemed uneven and disrupted, and the interstitial space was expanded by many collagen bundles and macrophages (Figure 7c-e). TEM of lung tissues of rats from groups 3 and 4 showed amelioration in type II pneumocytes and normal alveolar septum (Figure 8a-d). Type II pneumocytes with apical short microvilli showed improvement in the cytoplasm and lamellar bodies in group 3 (Figure 8a). In addition, a normal thin

Table IV. Changes in the area percentage of COX-2, TNF-α, and p53 immunopositivity in all studied groups.

Groups	COX-2 Area %	TNF-α Area %	p53 Area %
Normal control	5.10 ± 0.75^a	1.77 ± 0.22^a	2.10 ± 0.18^a
CCl4	32.79 ± 1.83^d	30.02 ± 1.16^c	31.75 ± 1.10^c
CCl4 + rat BM-MSCs	9.91 ± 0.97^b	2.98 ± 0.56^a	4.00 ± 0.61^a
CCl4 + mouse BM-MSCs	17.63 ± 1.26^c	6.35 ± 0.15^b	11.33 ± 0.12^b
F-probability		$p < 0.05$	

Results are displayed as mean ± SE. There are six animals in each group. Mean values with different superscript letters are significantly different at $p < 0.05$. [a,b,c,d]Indicated the similarity or difference between groups. Bone marrow-derived mesenchymal stem cells (BM-MSCs), cyclooxygenase (COX)-2, tumor necrosis factor-α (TNF-α).

11392

part of the inter-alveolar septum was observed (Figure 8b). In group 4, the amelioration of type II pneumocytes with a nucleus and lamellar bodies and the thick part of the inter-alveolar septum were depicted (Figure 8c-d).

Discussion

The present study evaluated the protective effect of rat or mouse BM-MSCs against CCl4-induced oxidative stress in rat lung tissues. CCl4 is
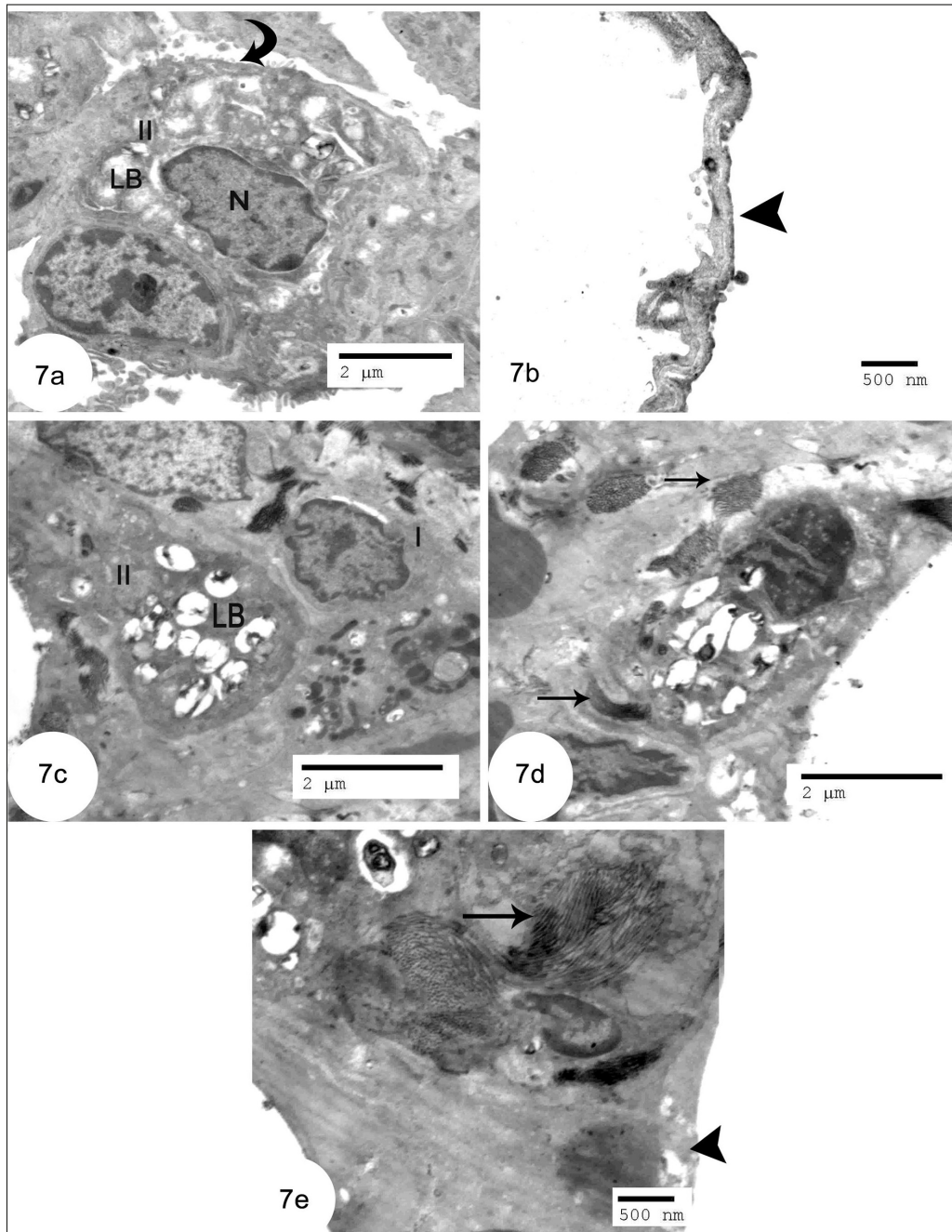
Figure 7. The lung of a healthy rat is depicted in an electron micrograph (**a**) with Type II pneumocytes (II) with nuclei (N), lamellar bodies (LB), and the free surface coated with short microvilli (arrow curved). **b**, Notice the thin part of the inter-alveolar septum (*arrowhead*) (Scale bar of **a** = 2 μm, Scale bar of **b** = 500 nm. **c-e**, CCl4 group showing Type II pneumocytes with vacuolated lamellar bodies (LB). Notice marked thickening of the interalveolar septum (*arrowhead*) that contains bundles of collagen fibers (arrow long) [Scale bar of (**c-d**) = 2 μm, Scale bar of (**e**) = 500 nm].

a poisonous chemical found in numerous tissues, including the lungs. It is broken down into two metabolites (CCl_3 and CCl_3O_2) by the cytochrome P450 enzyme; CCl_3 reacts quickly with O_2 and produces reactive free radicals[39].

As a result of the action of the phase 1 enzyme that is mediated by mitochondrial cytochrome P-450, CCl4 is bio-catabolized into free radicals, CCl_3 and CCl_3O_2. Normally, the free radicals are subjected to detoxification and neutralization by the phase 2 enzymes (GST) and antioxidant enzymes (SOD, GPx and catalase). The exacerbated production of the free radicals and ROS activates the process of LPO and depletes GSH, which is replenished by glutathione reductase and is used as a substrate for GST and GPx. Thus, CCl4 exposure results in an increase in oxidative stress and exhaustion of the antioxidant defense system[40-42].

In the current study, rats treated with CCl4 had significantly lower levels of SOD, GSH, GPx, and GST in their lung tissues than rats in the normal control group, but their LPO product levels were significantly increased. These findings concur with those published by Ganie et al[43] in 2010. The elevated LPO and the decrease in the antioxidant defense system may be due to the inactivation of the anti-oxidative enzymes such as SOD, GPx, GR, and GST, as well as the depletion in the GSH content in the lung tissues of the CCl4-treated
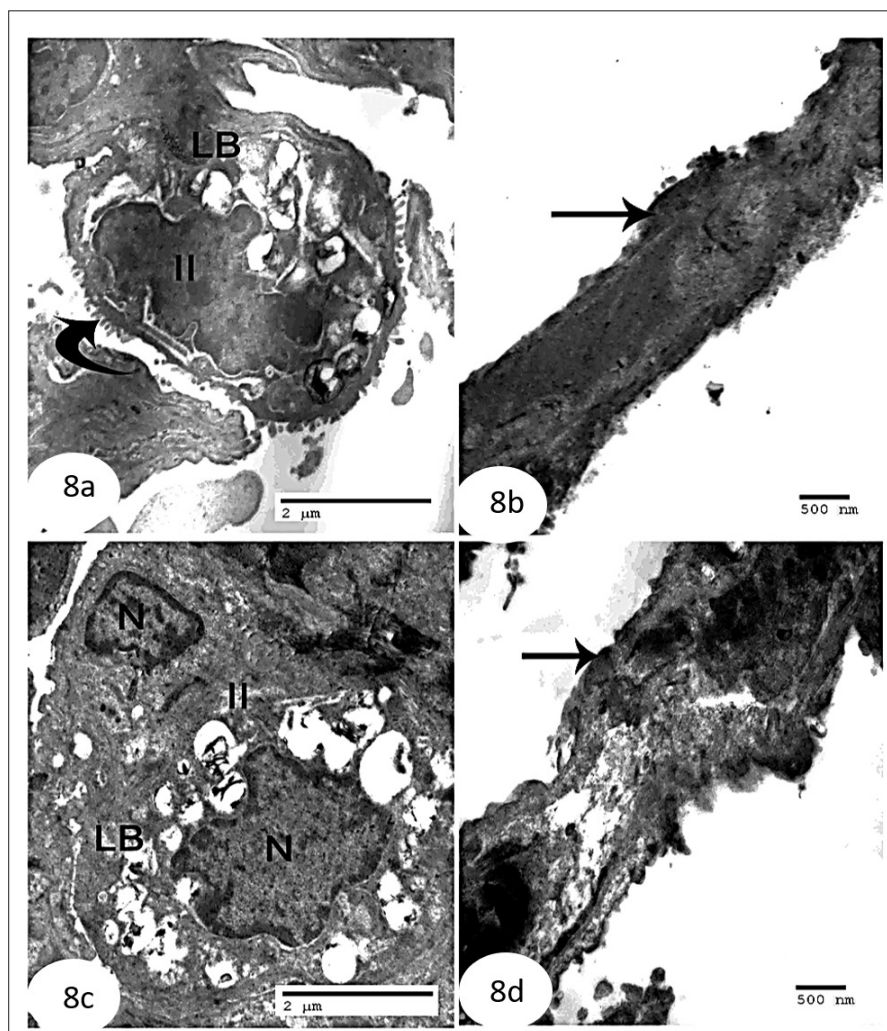
Figure 8. Electron micrograph of a section of lung of CCl4 + rat BM-MSCs treated groups (**a**) showing marked improvement of Type II pneumocytes (II) lamellar bodies (LB), and free surface with short microvilli (curved arrow). **b**, Normal thin part of inter-alveolar septum (*long arrow*) [Scale bar of (**a**) = 2 μm, Scale bar of (**b**) = 500 n]. **c-d**, CCl4 + mouse BM-MSCs showing amelioration of Type II pneumocytes (II) with nucleus (N) and mild thick part of interalveolar septum (*long arrow*) [Scale bar of (**c**) = 2 μm, Scale bar of (**d**) = 500 nm

rats[39,43,44]. In the present study, the treatment with rat and mouse BM-MSCs significantly decreased the lung LPO and restored the SOD, GPx, and GST activities and GSH content in the CCl4-treated rats. Furthermore, the treatment with rat BM-MSCs was more effective in reducing oxidative stress and enhancing the antioxidant defense system when compared to that with mouse BM-MSCs.

It is worth mentioning that the excess production of ROS from mitochondria activates the intrinsic pathway of apoptosis through an increase in the expression of the proapoptotic protein, p53, which leads to the activation of caspase-3 and apoptosis. The increased oxidative stress in CCl4-injected rats in the present study may activate the apoptotic process through stimulation of this pathway in addition to the extrinsic signaling pathway triggered by binding TNF-α to its receptor, tumor necrosis factor receptor (TNFR) (Figure 9).

In the present study, the intravenous infusion of BM-MSCs to CCl4-intoxicated rats significantly decreased the elevated expression of inflammatory mediators COX-2 and TNF-α in lung tissue; the effect of rat BM-MSCs was more potent. The anti-inflammatory effects of BM-MSCs may be secondary to the suppression of oxidative stress and enhancement of the antioxidant defense system (Figure 9), as evidenced in the results of the present investigation. These results are in accordance with Thum et al[45], who suggested that MSCs have anti-inflammatory and immunomodulatory capabilities. The antioxidant and anti-inflammatory effects of MSCs may play some crucial roles in the protection and treatment of organs from various toxicological causes such as CCl4-intoxication, preserving organ function in the process.

Light microscopic examinations of the H&E-stained sections of the lungs in Group 2 revealed the presence of hemorrhage, damaged alveoli, alveolar edema, and inflammatory cells. These findings are in accordance with another study[5], which showed that alveolar septa degeneration, connective tissue and elastic fiber disruption, and capillary congestion were all brought on by CCl4. The rupture of the alveolar walls and bronchioles, the aggregation of fibroblasts, and the disarray of Clara cells, among other traumas, were some of the histological abnormalities in the lung tissues of CCl4-treated rats, according to Naz et al[46]. The present study also revealed that sections from rats in Group 3 displayed a normal histological architecture of the lung, whereas those from Group 4 showed rupture of the alveolar walls. The severity of tissue damage in Group 4 was higher than that in Group 3, suggesting that rat BM-MSCs provide higher protection than mouse BM-MSCs. In concordance with the present study, Gao et al[47] reported decreases in several pulmonary histopathological changes following treatment with MSCs in a bleomycin-induced acute lung injury rat model. Moreover, Lai et al[48] demonstrated the protective effect of MSC in a rat model of ventilator-induced lung injury *via* the suppression of the polymorphonuclear neutrophil activation. It is worth mentioning that reactive oxygen species (ROS) generated from CCl4 are said to cause oxidative damage in the lungs of rats (Figure 9), perhaps through changing the status of the antioxidant enzymes, according to El-Aarag et al[5]. Catalase, peroxidase, and SOD are a few examples of antioxidant enzymes that are crucial in preventing free radical damage to lung tissues[38]. In accordance with these publications, the present study revealed a significant decrease in lung LPO and a significant elevation of lung GSH content and SOD, GST and GPx activities by treatment with allogenic and xenogenic BM-MSCs in association with the improvement of lung structural and histological integrity; the treatment with allogenic (rat) BM-MSCs was more effective. Thus, it can be elucidated that the improvements in the lung histopathological lesions could be attributed to the suppression of oxidative stress and enhancement of the antioxidant defense system.

Numerous animal studies[49-51] have thoroughly examined the physiological roles of MSCs, in particular chemotaxis. MSCs can go to areas of tissue damage and release angiogenic, anti-apoptotic, and anti-inflammatory substances such as stromal-derived factor-1 (SDF-1), transforming growth factor (TGF), vascular endothelial growth factor (VEGF), platelet-derived growth factor (PDGF), and hepatocyte growth factor (HGF) to inhibit the immune system. This promotes angiogenesis, which creates a safe environment for host cell repair and allows the wounded tissue to be preserved or restored after destruction.

In the current study, minimal collagen deposition was observed in sections from the control group; the lungs from Group 2 displayed extensive collagen deposition, whereas those from Groups 3 and 4 displayed reduced collagen deposition compared to those in Group 2. The results of the morphometrical and statistical analyses supported these conclusions. The % area of collagen stained with trichrome was found to rise sig-

nificantly in Group 2, with remarkable improvements in Groups 3 and 4 compared to Group 2. Similar findings were reported by Pääkkö et al[52], wherein acute and chronic CCl4 intoxication caused increased collagen deposition in the lungs due to free radical-mediated LPO.

Although the exact mechanism by which CCl4 causes fibrosis is still unclear, numerous types of pulmonary fibrosis, such as bronchiolitis obliterans, radiation, particulate matter, drugs (such as bleomycin), and chronic graft-versus-host-induced pulmonary fibrosis, have been successfully modeled and studied in rodents. In some circumstances, inflammatory mediators seem to be involved in the beginning and development of pulmonary fibrosis[53]. In mice, pulmonary fibrosis develops when the cytokine TNF-α is overexpressed[54]. Macrophages and other cell types release TNF-α in the lungs after exposure to pollutants such as asbestos and antibiotics such as bleomycin[55]. According to one study[56], the injection of MSCs decreased the amount of bleomycin-induced inflammation and collagen deposition within the lung tissue. MSCs can secrete a wide range of arteriogenic cytokines and contribute to reducing fibrosis through paracrine pathways[57].

Sections from rats in the control group displayed negative immunoreactivity, whereas those in Group 2 showed strong positive immunoreactivity for COX-2 and TNF-α in the current study. Treatment with rat and mouse BM-MSCs resulted in significant decreases in the levels of these markers when compared to those observed in Group 2. Furthermore, treatment with rat BM-MSCs was more effective in decreasing the expression levels of COX-2 and TNF-α when compared to that with mouse BM-MSCs. Similar findings were reported by Aslan et al[58], wherein increased expression levels of nuclear factor kappa B (NF-κB), COX-2, COX-1, and MDA were observed in CCl4-induced rats.

TNF-α causes tissue injury by enhancing the migration of neutrophils to the site of injury, increasing the production of proteolytic enzymes, and causing the generation of ROS[59]. Additionally, TNF-α induces apoptosis through extrinsic pathway (Figure 9) and causes tissue damage by directly stimulating the caspase pathway[60]. It is known to cause lung toxicity due to inflammation and *via* medications or other chemical compounds. In the present study, the treatment of CCl4-intoxicated rats with rat and mouse BM-MSCs produced a significant decrease in the elevated TNF-α; the treatment with rat BM-

MSCs was more effective. These results are in concurrence with Xiao and Xie[61], who reported that MSCs can suppress the release of pro-inflammatory factors and reduce inflammatory injury. It was also revealed by a past publication[62] that the treatments of rats with MSCs and MSC-derived exosomes provide protection against intestinal ischemia-reperfusion acute lung injury, and the expression levels of TNF-α were substantially lower. Furthermore, Song et al[63] demonstrated that MSCs and MSCs-derived exosome treatment effectively inhibits chronic allergic airway inflammation.

The transcriptional factor p53 is the key subunit of the p53 signaling pathway and is reported[64] to be involved in lung apoptosis (Figure 9). The current study showed that p53 was significantly upregulated in the lungs of the CCl4-treated rats. Treatment with BM-MSCs restored these aberrant parameters, suggesting that MSCs mediated the attenuation of apoptosis against CCl4-induced lung injury (Figure 9). Treatment of CCl4-injected rats with rat and mouse BM-MSCs resulted in a significant decrease in the apoptotic protein, p53, when compared to that observed in Group 2. In support of these results, the histological investigations of lungs in the current study indicated a decrease in the number of apoptotic cells and the score of apoptosis in groups 3 and 4 when compared to group 2. The lungs of CCl4-injected rats depicted the presence of many apoptotic cells and apoptotic bodies and remnants, while CCl4-injected rats treated with rat and mouse BM-MSCs showed a reduced number.

Lung sections from patients with idiopathic pulmonary fibrosis were positively stained for p53, whereas those from normal subjects did not demonstrate any immunoreactivity[65]. This is in agreement with the results of the current study, wherein lung sections from Group 2 showed strong positive immunoreaction for p53, whereas those from Group 1 (control) did not show any reaction. Treatment with BM-MSCs improved the level of immunoreaction in the pulmonary cells.

The fibrotic changes that occurred in the CCl4-treated rats were confirmed by electron microscopic examinations of the lung sections, which revealed the thickening of the inter-alveolar septum and the presence of bundles of collagen fibers. Fewer lamellar bodies were noted, which emphasized the disruption of surfactant synthesis. Although details about the process-

ing of the surfactant remain poorly understood, a decrease in the number of mature lamellar bodies indicates disruption of the process.

In the current study, BM-MSCs derived from rats were more effective than those derived from mice. This may be attributed to the fact that xenogeneic MSCs are associated with inferior results compared to autogenous MSCs. Niemeyer et al[66] reported that the application of xenogeneic MSCs to a critical-size bone defect model resulted in a significant decrease in bone formation compared to that observed after the application of autogenous MSCs. According to this last publication, while the autogenous MSCs led to increased healing of critical-size bone defects, it was not possible to demonstrate analogous effects for the xenogeneic transplantation of MSCs.

In humans, idiopathic pulmonary fibrosis has been demonstrated[67-69] to be caused by damage to alveolar epithelial cells due to genetic, environmental and immunological factors. This damage in epithelial cells results in the formation of profibrotic factors, which then cause migration, proliferation, differentiation of fibroblasts and myofibroblasts, and the accumulation of extracellular matrix, thereby resulting in pulmonary fibrosis. Several factors, including exposures to toxic chemicals such as CCl4 and others, contribute to the development of idiopathic pulmonary fibrosis[67]. The present study provides evidence for the potential effects of allogeneic (rats) MSCs and xenogeneic (mice) MSCs to prevent rat lung damage and fibrosis; allogeneic or autogenous MSCs were more potent. These experimental results may help to predict similar effects of MSCs on the progress of pulmonary fibrosis in humans. However, further clinical studies on human beings are required to confirm these predictions. This experimental study may also help to suggest the mechanisms of actions of MSCs that prevent and cure lung damage and fibrosis (Figure 9).

Figure 9. Schematic figure showing the modes of actions of BM-MSCs to reduce lung inflammation, cell death, fibrosis and cirrhosis.

Conclusions

The findings of this study indicate that CCl4 induced oxidation stress, which activated the intrinsic apoptosis *via* the increased expression of p53 and stimulated the inflammatory process through the NF-κB pathway. The activation of NF-κB resulted in an increase in the production of inflammatory cytokines such as TNF-α and COX-2. Increased levels of TNF-α can activate apoptosis through an extrinsic pathway by binding to the TNF receptor. Elevations in TNF-α levels and LPO can lead to cell necrosis (Figure 9). Treatment with both rat and mouse BM-MSCs improved CCl4-induced lung dysfunction and injury by targeting the mediators of oxidative stress, apoptosis, necrosis, and inflammation, as indicated in Figure 9.

Conflict of Interest
The authors declare that they have no conflict of interests.

Ethics Approval
All animals' procedures were conducted in accordance with the ethical guidelines for the use and care of animal of the Experimental Animal Ethics Committee, Faculty of Science, Beni-Suef University, Egypt (Ethical Approval Number BSU/FS/ 2019-73). All efforts were done to reduce the number and suffering of animals.

Authors' Contribution
Conceptualization, M.A., S.H.A. and O.M.A.; methodology, A.A., M.A., and O.M.A.; software, A.A.; validation, A.A., M.A., S.H.A., F.A.J., F.S.A. and O.M.A.; formal analysis, A.A.; investigation, A.A., M.A., S.H.A., F.A.J., F.S.A. and O.M.A.; resources, A.A.,F.A.J. and F.S.A.; data curation, A.A., M.A. and O.M.A.; writing-original draft preparation, A.A. M.A., S.H.A. and O.M.A.; writing-review and editing A.A., M.A., S.H.A., F.A.J., F.S.A. and O.M.A; visualization, A.A., M.A., S.H.A., F.A.J., F.S.A. and O.M.A; supervision, M.A., S.H.A. and O.M.A; project administration, M.A., S.H.A., F.A.J., F.S.A. and O.M.A; funding acquisition, A.A., F.A.J. and F.S.A. All authors have read and agreed to the published version of the manuscript.

Availability of Data and Materials
The data are available from the corresponding author upon reasonable request.

Informed Consent
Not applicable.

ORCID ID
A. Adel: 0000-0002-7362-7362-6392
M. Abdul-Hamid: 0000-0002-0877-3097
S.H. Abdel-Kawi: 0000-0002-7284-0856
N.S. Abd El-Gawaad: 0000-0001-5606-3906
O.M. Ahmed: 0000-0003-3781-9709

References

1) Dong S, Chen QL, Song YN, Sun Y, Wei B, Li XY, Hu YY, Liu P, Su SB. Mechanisms of CCl4-induced liver fibrosis with combined transcriptomic and proteomic analysis. J Toxicol Sci 2016; 41: 561-572.

2) Khan RA, Khan MR, Sahreen S, Bokhari J. Prevention of CCl4-induced nephrotoxicity with Sonchus asper in rat. Food Chem Toxicol 2010; 48: 2469-2476.

3) Said ES, Mohammed AH, Ali HM, Babiker AY, Alnughaymishi R, Althaqeel NZ, Ahmed AS. Evaluation of hepatoprotective effect of Nebivolol and sodium copper Chlorophyllin on CCL4-induced hepatotoxicity in mice. Eur Rev Med Pharmacol Sci 2022; 26: 1717-1728.

4) Hameed H, Farooq M, Vuillier C, Piquet-Pellorce C, Hamon A, Dimanche-Boitrel MT, Samson M, Le Seyec J. RIPK1 in liver parenchymal cells limits murine hepatitis during acute CCl4-Induced liver injury. Int J Mol Sci 2022; 23: 7367.

5) El-Aarag B, Attia A, Zahran M, Younes A, Tousson E. New phthalimide analog ameliorates CCl4 induced hepatic injury in mice via reducing ROS formation, inflammation, and apoptosis. Saudi j biol Sci 2021; 28: 6384-6395.

6) Ahmad B, Khan MR, Shah NA. Amelioration of carbon tetrachloride-induced pulmonary toxicity with Oxalis corniculata. Toxicol Ind Health 2015; 31: 1243-1251.

7) Khan RA. Protective effect of Launaea procumbens (L.) on lungs against CCl 4-induced pulmonary damages in rat. BMC Complement Altern Med 2012; 12: 1-7.

8) Jiang L, Huang J, Wang Y, Tang H. Metabonomic analysis reveals the CCl4-induced systems alterations for multiple rat organs. J Proteome Res 2012; 11: 3848-3859.

9) Mizuguchi S, Takemura S, Minamiyama Y, Kodai S, Tsukioka T, Inoue K, Okada S, Suehiro S. S-allyl cysteine attenuated CCl4-induced oxidative stress and pulmonary fibrosis in rats. Biofactors 2006; 26: 81-92.

10) Anttinen H, Oikarinen A, Puistola U, Pääkkö P, Ryhänen L. Prevention by zinc of rat lung collagen accumulation in carbon tetrachloride injury. Am Rev Respir Dis 1985; 132: 536-5340.

11) Pääkkö P, Sormunen R, Risteli L, Risteli J, Ala-Kokko L, Ryhänen L. Malotilate prevents accumulation of type III pN-collagen, type IV collagen, and laminin in carbon tetrachloride-induced pulmonary fibrosis in rats. Am J Respir Crit Care Med 1989; 139: 1105-1111.

12) Chambers DC, Enever D, Lawrence S, Sturm MJ, Herrmann R, Yerkovich S, Musk M, Hopkins PM. Mesenchymal stromal cell therapy for chronic lung allograft dysfunction: results of a first-in-man study. Stem Cells Transl Med 2017; 6: 1152-1157.

13) Prockop DJ, Gregory CA, Spees JL. One strategy for cell and gene therapy: harnessing the power of adult stem cells to repair tissues. Proc Natl Acad Sci 2003; 100: 11917-11923.

14) François S, Bensidhoum M, Mouiseddine M, Mazurier C, Allenet B, Semont A, Frick J, Saché A, Bouchet S, Thierry D, Gourmelon P. Local irradiation not only induces homing of human mesenchymal stem cells at exposed sites but promotes their widespread engraftment to multiple organs: a study of their quantitative distribution after irradiation damage. Stem Cells 2006; 24: 1020-1029.

15) Wang R, Zhu CZ, Qiao P, Liu J, Zhao Q, Wang KJ, Zhao TB. Experimental treatment of radiation pneumonitis with human umbilical cord mesenchymal stem cells. Asian Pac J Trop Med 2014; 7: 262-266.

16) Tsuchiya A, Takeuchi S, Watanabe T, Yoshida T, Nojiri S, Ogawa M, Terai S. Mesenchymal stem cell therapies for liver cirrhosis: MSCs as "conducting cells" for improvement of liver fibrosis and regeneration. Inflamm Regen 2019; 39: 1-6.

17) Bonfield TL, Caplan AI. Adult mesenchymal stem cells: an innovative therapeutic for lung diseases. Discov Med 2010; 9: 337-345.

18) Inamdar AC, Inamdar AA. Mesenchymal stem cell therapy in lung disorders: pathogenesis of lung diseases and mechanism of action of mesenchymal stem cell. Exp Lung Res 2013; 39: 315-327.

19) Lan YW, Choo KB, Chen CM, Hung TH, Chen YB, Hsieh CH, Kuo HP, Chong KY. Hypoxia-preconditioned mesenchymal stem cells attenuate bleomycin-induced pulmonary fibrosis. Stem Cell Res Ther 2015; 6: 1-7.

20) da Silva Meirelles L, Fontes AM, Covas DT, Caplan AI. Mechanisms involved in the therapeutic properties of mesenchymal stem cells. Cytokine Growth Factor Rev 2009; 20: 419-427.

21) Akram KM, Samad S, Spiteri MA, Forsyth NR. Mesenchymal stem cells promote alveolar epithelial cell wound repair in vitro through distinct migratory and paracrine mechanisms. Resp Res 2013; 14: 1-6.

22) Ahmed OM, Hassan MA, Saleh AS. Combinatory effect of hesperetin and mesenchymal stem cells on the deteriorated lipid profile, heart and kidney functions and antioxidant activity in STZ-induced diabetic rats. Biocell 2020; 44: 27-29.

23) Ahmed EA, Ahmed OM, Fahim HI, Ali TM, Elesawy BH, Ashour MB. Potency of bone marrow-derived mesenchymal stem cells and indomethacin in complete Freund's adjuvant-induced arthritic rats: roles of TNF-α, IL-10, iNOS, MMP-9, and TGF-β1. Stem Cells Int 2021; 2021: 1-1.

24) Chaudhary JK, Rath PC. Microgrooved-surface topography enhances cellular division and proliferation of mouse bone marrow-derived mesenchymal stem cells. PLoS One 2017; 12: e0182128.

25) Abd-Allah GA, El-Bakry KA, Bahnasawy MH, El-Khodary ES. Protective effects of curcumin and ginger on liver cirrhosis induced by carbon tetrachloride in rats. Int J Pharmacol 2016; 12: 361-369.

26) Mohamed TA, Abouel-Nour MF, Eldemerdash R, Elgalady DA. Therapeutic effects of bone marrow stem cells in diabetic rats. J Comput Sci Syst Boil 2016; 9: 58-68.

27) Preuss HG, Jarrell ST, Scheckenbach R, Lieberman S, Anderson RA. Comparative effects of chromium, vanadium and Gymnema sylvestre on sugar-induced blood pressure elevations in SHR. J Am Coll Nutr 1998; 17: 116-123.

28) Yagi K. Lipid peroxides and human disease. Chem Phys Lipids 1987; 45: 337-351.

29) Matkovics B, Kotorman M, Varga IS, Hai DQ, Varga C. Oxidative stress in experimental diabetes induced by streptozotocin. Acta Physiol Hung 1998; 85: 29-38.

30) Marklund S, Marklund G. Involvement of the superoxide anion radical in the autoxidation of pyrogallol and a convenient assay for superoxide dismutase. European J Biochem 1974; 47: 469-474.

31) Beutler E, Duron O, Kelly BM. Improved method for the determination of blood glutathione. J Lab Clin Med 1963; 61: 882-888.

32) Mannervik B, Guthenberg C. Glutathione transferase (human placenta). In: Methods in Enzymology 1981; 77: 231-235. Academic Press.

33) Bancroft J, Gamble M. Theory and Practice of Histological Techniques. 5th Edn, Edinburg. Churchill Livingstone Pup., 2002; pp. 172-175.

34) Suvarna SK, Layton C, Bancroft JD. Bancroft's theory and practice of histological techniques, 7th Edn 2013; Elsevier, Churchilli Livingstone, England.

35) Cemek M, Kağa S, Şimşek N, Büyükokuroğlu ME, Konuk M. Antihyperglycemic and antioxidative potential of Matricaria chamomilla L. in streptozotocin-induced diabetic rats. J Nat Medi 2008; 62: 284-293.

36) Arsad SS, Esa NM, Hamzah H. Histopathologic changes in liver and kidney tissues from male Sprague Dawley rats treated with Rhaphidophora decursiva (Roxb.) Schott extract. J Cytol Histol S 2014; 4: 1-6.

37) Bozzola JJ, Russell LD. Electron microscopy: principles and techniques for biologists. Jones & Bartlett Learning; 1999.

38) Aslan A, Gok O, Erman O, Kuloglu T. Ellagic acid impedes carbontetrachloride-induced liver damage in rats through suppression of NF-κB, Bcl-2 and regulating Nrf-2 and caspase pathway. Biomed Pharmacother 2018; 105: 662-669.

39) Ganie SA, Haq E, Hamid A, Qurishi Y, Mahmood Z, Zargar BA, Masood A, Zargar MA. Carbon tetrachloride induced kidney and lung tissue damages and antioxidant activities of the aqueous rhizome extract of Podophyllum hexandrum. BMC Complement Altern Med 2011; 11: 17.

40) Wu CY, Weng YM, Liu CT, Chuang PT, Liu SY, Tseng CY. Hepatoprotective and antioxidative properties of Chinese herbal medicine xiao-chai-hu-tang formulated with Bupleurum kaoi Liu on carbon tetrachloride-induced acute hepatotoxicity in rats. J Food Drug Anal 2010; 18: 3.

41) Seung KR, Jung KH. Protective Effect of curcumin and aqueous extract of onchengyeum on CCl 4-induced hepatotoxicity. Biomol Ther 2005; 13: 232-239.

42) Lee GH, Lee HY, Choi MK, Chung HW, Kim SW, Chae HJ. Protective effect of Curcuma longa L. Extract on CCl 4-induced acute hepatic stress. BMC Res Notes 2017; 10: 1-9.

43) Ganie SA, Haq E, Masood A, Zargar MA. Amelioration of carbon tetrachloride induced oxidative stress in kidney and lung tissues by ethanolic rhizome extract of Podophyllum hexandrum in Wistar rats. J Med Plants Res 2010; 4: 1673-1677.

44) Kurt A, Tumkaya L, Yuce S, Turut H, Cure MC, Sehitoglu I, Kalkan Y, Pusuroglu G, Cure E. The protective effect of infliximab against carbon tetrachloride-induced acute lung injury. Iran J Basic Med Sci 2016; 19: 685-691.

45) Thum T, Bauersachs J, Poole-Wilson PA, Volk HD, Anker SD. The dying stem cell hypothesis: immune modulation as a novel mechanism for progenitor cell therapy in cardiac muscle. J Am Coll Cardiol 2005; 46: 1799-1802.

46) Naz K, Khan MR, Shah NA, Sattar S, Noureen F, Awan ML. Pistacia chinensis: a potent ameliorator of CCl$_4$ induced lung and thyroid toxicity in rat model. Biomed Res Int 2014; 2014: 192906.

47) Gao F, Li Q, Hou L, Li Z, Min F, Liu Z. Mesenchymal stem cell-based angiotensin-converting enzyme 2 in treatment of acute lung injury rat induced by bleomycin. Exp Lung Res 2014; 40: 392-403.

48) Lai TS, Wang ZH, Cai SX. Mesenchymal stem cell attenuates neutrophil-predominant inflammation and acute lung injury in an in vivo rat model of ventilator-induced lung injury. Chin Med J 2015; 128: 361-367.

49) Alimperti S, You H, George T, Agarwal SK, Andreadis ST. Cadherin-11 regulates both mesenchymal stem cell differentiation into smooth muscle cells and the development of contractile function in vivo. J Cell Sci 2014; 127: 2627-2638.

50) Ulivi V, Tasso R, Cancedda R, Descalzi F. Mesenchymal stem cell paracrine activity is modulated by platelet lysate: induction of an inflammatory response and secretion of factors maintaining macrophages in a proinflammatory phenotype. Stem Cells Dev 2014; 23: 1858-1869.

51) Linero I, Chaparro O. Paracrine effect of mesenchymal stem cells derived from human adipose tissue in bone regeneration. PloS one 2014; 9: e107001.

52) Pääkkö P, Anttila S, Sormunen R, Ala-Kokko L, Peura R, VJ, Ryhänen L. Biochemical and morphological characterization of carbon tetrachloride-induced lung fibrosis in rats. Arch Toxicol 1996; 70: 540-552.

53) Bringardner BD, Baran CP, Eubank TD, Marsh CB. The role of inflammation in the pathogenesis of idiopathic pulmonary fibrosis. Antioxid Redox Signal 2008; 10: 287-301.

54) Miyazaki Y, Araki K, Vesin C, Garcia I, Kapanci Y, Whitsett JA, Piguet PF, Vassalli P. Expression of a tumor necrosis factor-alpha transgene in murine lung causes lymphocytic and fibrosing alveolitis. A mouse model of progressive pulmonary fibrosis. J Clin Invest 1995; 96: 250-259.

55) Zhang Y, Lee TC, Guillemin B, Yu MC, Rom WN. Enhanced IL-1 beta and tumor necrosis factor-alpha release and messenger RNA expression in macrophages from idiopathic pulmonary fibrosis or after asbestos exposure. J Immunol 1993; 150: 4188-4196.

56) Ortiz LA, Gambelli F, McBride C, Gaupp D, Baddoo M, Kaminski N, Phinney DG. Mesenchymal stem cell engraftment in lung is enhanced in response to bleomycin exposure and ameliorates its fibrotic effects. Proc Natl Acad Sci 2003; 100: 8407-8411.

57) Kinnaird T, Stabile E, Burnett MS, Shou M, Lee CW, Barr S, Fuchs S, Epstein SE. Local delivery of marrow-derived stromal cells augments collateral perfusion through paracrine mechanisms. Circulation 2004; 109: 1543-1549.

58) Aslan A, Hussein YT, Gok O, Beyaz S, Erman O, Baspinar S. Ellagic acid ameliorates lung damage in rats via modulating antioxidant activities, inhibitory effects on inflammatory mediators and apoptosis-inducing activities. Environ Sci Pollut Res Int 2020; 27: 7526-7537.

59) Mukhopadhyay S, Hoidal JR, Mukherjee TK. Role of TNFα in pulmonary pathophysiology. Respir Res 2006; 7: 1-9.

60) Elmore S. Apoptosis: a review of programmed cell death. Toxicol Pathol 2007; 35: 495-516.

61) Xiao K, Xie LX. Advances in mesenchymal stem cell-mediated tissue repair of lung injury. Chronic Dis Transl Med 2021; 7: 75-78.

62) Liu J, Chen T, Lei P, Tang X, Huang P. Exosomes Released by Bone Marrow Mesenchymal Stem Cells Attenuate Lung Injury Induced by Intestinal Ischemia Reperfusion via the TLR4/NF-κB Pathway. Int J Med Sci 2019; 16: 1238-1244. Erratum in: Int J Med Sci. 2023; 20: 1114.

63) Song J, Zhu XM, Wei QY. MSCs reduce airway remodeling in the lungs of asthmatic rats through

the Wnt/β-catenin signaling pathway. Eur Rev Med Pharmacol Sci 2020; 24: 11199-11211.

64) Chillemi G, Kehrloesser S, Bernassola F, Desideri A, Dötsch V, Levine AJ, Melino G. Structural evolution and dynamics of the p53 proteins. Cold Spring Harb Perspect Med 2017; 7: a028308.

65) Disayabutr S, Kim EK, Cha SI, Green G, Naikawadi RP, Jones KD, Golden JA, Schroeder A, Matthay MA, Kukreja J, Erle DJ. miR-34 miRNAs regulate cellular senescence in type II alveolar epithelial cells of patients with idiopathic pulmonary fibrosis. PloS One 2016; 11: e0158367.

66) Niemeyer P, Szalay K, Luginbühl R, Südkamp NP, Kasten P. Transplantation of human mesenchymal stem cells in a non-autogenous setting for bone regeneration in a rabbit critical-size defect model. Acta Biomater 2010; 6: 900-908.

67) Kletukhina S, Mutallapova G, Titova A, Gomzikova M. Role of Mesenchymal Stem Cells and Extracellular Vesicles in Idiopathic Pulmonary Fibrosis. Int J Mol Sci 2022; 23: 11212.

68) Yang S, Liu P, Jiang Y, Wang Z, Dai H, Wang C. Therapeutic applications of mesenchymal stem cells in idiopathic pulmonary fibrosis. Front Cell Dev Biol 2021; 9: 639657.

69) Samarelli AV, Tonelli R, Heijink I, Martin Medina A, Marchioni A, Bruzzi G, Castaniere I, Andrisani D, Gozzi F, Manicardi L, Moretti A. Dissecting the role of mesenchymal stem cells in idiopathic pulmonary fibrosis: cause or solution. Front Pharmacol 2021; 12: 692551.